

Development of IGZO TFTs and Their Applications to Next-Generation Flat-Panel Displays

Hsing-Hung Hsieh, Hsiung-Hsing Lu, Hung-Che Ting, Ching-Sang Chuang, Chia-Yu Chen and Yusin Lin

Abstract

Organic light-emitting devices (OLEDs) have shown superior characteristics and are expected to dominate the next-generation flat-panel displays. Active-matrix organic light-emitting diode (AMOLED) displays, however, have stringent demands on the performance of the backplane. In this paper, the development of thin-film transistors (TFTs) based on indium gallium zinc oxide (IGZO) on both Gen 1 and 6 glasses, and their decent characteristics, which meet the AMOLED requirements, are shown. Further, several display prototypes (e.g., 2.4" AMOLED, 2.4" transparent AMOLED, and 32" AMLCD) using IGZO TFTs are demonstrated to confirm that they can indeed be strong candidates for the next-generation TFT technology not only of AMOLED but also of AMLCD (active-matrix liquid crystal display).

Keywords: oxide TFT, IGZO, AMOLED, transparent display, AMLCD

1. Introduction

Much effort has been exerted to develop organic light-emitting devices (OLEDs) since the thin-film multilayer-structure electroluminescence device based on an organic emitter was reported [1]. OLEDs show many attractive characteristics, such as Lambertian self-emission, high luminous efficiency and low operation voltage, light weight, broad color gamut, and low-temperature and large-area fabrication capability [2]. As such, the active-matrix organic light-emitting display (AMOLED) is expected to dominate the flat-panel display (FPD) industry in the near future.

As OLED is a current-controlled display device, however, the performance of the driving thin-film transistors (TFTs) is very important to achieve uniform brightness. The low-temperature polycrystalline silicon (LTPS) TFTs show high mobility and good stability, but its uniformity is typically not acceptable for AMOLED operation. The hydrogenated amorphous silicon (a-Si:H) TFTs have good uniformity, but their low mobility and poor stability also make them hardly applicable in AMOLED. Alternatively, oxide-based semiconductors with specific electronic configura-

tions have been widely investigated of late due to their merits, such as high mobility, high transparency, low processing temperature, and potentially good uniformity [3-12]. All these merits make oxide TFTs strong candidates for the AMOLED backplane.

On the other hand, the demands on the performance of FPDs are increasing. For example, the resolution and frame rate should become higher and higher even for the active-matrix liquid crystal display (AMLCD). Such demands exceed the limits of the performance of a-Si:H TFTs, the present working horses of AMLCD. Therefore, high-performance TFTs are also needed for the future AMLCD. The oxide TFTs are also strong candidates for the AMLCD backplane.

In this paper, the development and characteristics of oxide TFTs based on indium gallium zinc oxide (IGZO) are discussed to show their advantages for the future FPD. As the next-generation TFT technology, several display prototypes of oxide TFTs are demonstrated on small and large displays and on novel transparent displays, including a 2.4" AMOLED, a 2.4" transparent AMOLED, and a 32" AMLCD.

2. Characteristics of Oxide TFTs

Several types of bottom-gate IGZO TFTs with various configurations (e.g., coplanar, etch-stop, and back-channel etch types) were developed and fabricated using the fully

Manuscript Received November 12, 2010; Revised December 14, 2010; Accepted for publication December 15, 2010.

The authors would like to acknowledge all the members of the OLED technology division of AU Optronics Corporation for their kind discussion and cooperation.

Corresponding author: Yusin Lin

OLED Technology Div., AU Optronics Corp., Hsinchu, Taiwan

E-mail: Yusin.Lin@auo.com Tel: +886-3-500-8800 ext. 3368 Fax: +886-3-565-1840

conventional processes. The active layer was deposited via DC sputtering, which is adequate for large-area deposition. The devices with each structure show their own advantages and disadvantages, as partly described in Table 1. The coplanar and back-channel etching types need fewer photomasks and can be processed more easily. The etch stop type needs an extra photomask but has a good interface quality in both the front and back channels. Generally, near $10 \text{ cm}^2/\text{Vs}$ mobility, close to 0 V threshold voltage, and 0.2~0.3 V/decade subthreshold slope can be obtained. Unlike the local fluctuations typically observed in LTPS TFTs, the IGZO TFTs show very good short-range uniformity (standard variation of threshold voltage < 0.1 V within a $320 \times 400 \text{ mm}$ Gen 1 glass), which implies that perhaps no complex compensation circuit is needed for the AMOLED display pixel design. In addition, the IGZO TFTs show less than 0.1 V hysteresis, as can be seen in Fig. 1(a), which is also better than those of most LTPS TFTs and is believed to benefit AMOLED's image retention phenomenon. The DC bias stress stability of IGZO TFTs is shown in Fig. 1(b), and only slight variations were found for the transfer curves. Such decent performance not only is much better than that of the a-Si:H TFTs and compatible with that of the LTPS TFTs, but also renders IGZO TFTs suitable for the AMOLED backplane.

To investigate the influence of the back channel on the device performance, bottom-gate coplanar-type IGZO TFTs were fabricated with and without a channel protection layer. Fig. 2 shows the schematic structures of the coplanar-type IGZO TFTs that were studied in this work. The fabrication processes are fully compatible with the conventional TFT-LCD processes. As shown in Fig. 2(a), the Ti/Al/Ti trilayers

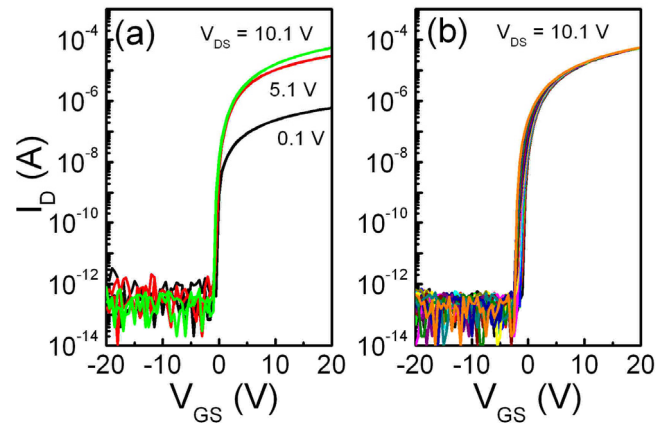


Fig. 1. (a) Typical transfer curves and hysteresis of IGZO TFTs. (b) Positive gate bias stress of $V_{GS} = 20 \text{ V}$ for 30,000 sec.

served as both the first metal layer (also as the gate electrode) and the second metal layer (also as the source and drain electrodes). The 300-nm SiN_x was deposited via plasma-enhanced chemical vapor deposition (PECVD) to serve as the gate insulator. A 50-nm amorphous IGZO channel layer was deposited via DC sputtering, and was patterned via wet etching. The composition of In:Ga:Zn was about 1:1:1, and the power density of the deposition was about $0.5 \text{ W}/\text{cm}^2$. A SiO_x passivation layer was then deposited by PECVD on IGZO and was etched via reactive ion etching (RIE) to expose the vias. Fig. 2(b) shows the other type of device structure that was studied in this work. The IGZO channel layer and a thin SiO_x channel protection layer were deposited successively, then the SiO_x layer was patterned via dry etching, and the IGZO layer, via wet etching. These two types are then compared to determine the influence of the back channel on the device performance.

Table 1. Structures and features of various bottom-gate oxide TFT configurations

| Type | Coplanar | Back-Channel Etch | Etch Stop |
|-----------|---|--|--|
| Structure | | | |
| Features | <ul style="list-style-type: none"> ✓ Fewer masks ✓ Easy process ✓ Front-channel interface damage | <ul style="list-style-type: none"> ✓ Fewer masks ✓ Most compatible with a-Si TFTs ✓ Back-channel interface damage | <ul style="list-style-type: none"> ✓ Successive deposition (good front-channel interface) ✓ Back-channel protection ✓ Complicated process |

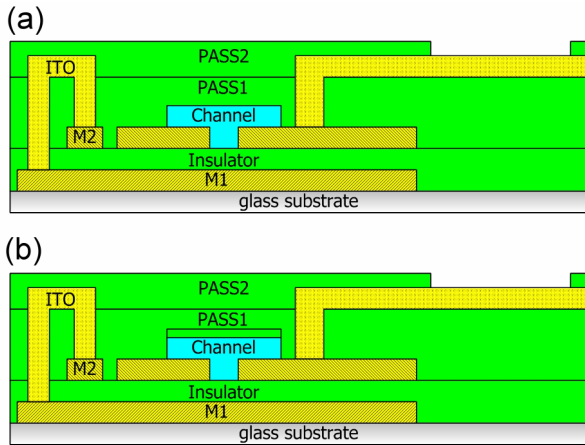


Fig. 2. Device structures of the IGZO TFTs (a) without and (b) with a channel protection layer.

Fig. 3 shows the typical electrical characteristics of the two types of IGZO TFTs. The channel width and length are 20 and 4 μm , respectively. Fig. 3(a) shows the transfer characteristics of the device without a SiO_x protection layer. The mobility (μ) is calculated to be 5.5 cm^2/Vs . The threshold voltage (V_t), which is defined by V_G at I_D of 1 nA and $V_{DS} = 10$ V, is -0.34 V. The subthreshold slope and the on/off current ratio are estimated to be 0.36 V/decade and $>10^7$, respectively. From the characteristics of the device with the SiO_x protection layer shown in Fig. 3(b), 6.2 cm^2/Vs mobility, -0.47 V threshold voltage, 0.19 V/decade subthreshold slope, and $>10^7$ on/off current ratio can be extracted. These extracted parameters are also summarized in Table 2. Although there is a negligible difference in threshold voltage between the two types of devices, the device with a SiO_x protection layer exhibits higher mobility and a

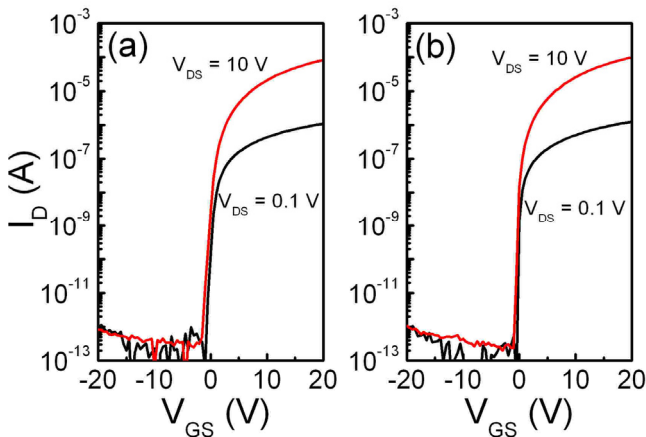


Fig. 3. Transfer characteristics of the IGZO TFTs (a) without and (b) with a channel protection layer.

Table 2. Summary of the parameters of the IGZO TFTs without and with a channel protection layer

| Type | Mobility (cm^2/Vs) | Threshold Voltage (V) | Subthreshold Slope (V/decade) | On/Off Ratio (A/A) |
|------------------------------------|--------------------------------------|-----------------------|-------------------------------|--------------------|
| Without a channel protection layer | 5.5 | -0.34 | 0.36 | $>10^7$ |
| With a channel protection layer | 6.2 | -0.47 | 0.19 | $>10^7$ |

distinctly smaller subthreshold slope. Accordingly, the subthreshold slope is related to the number of interface and bulk trap states [13]. A smaller subthreshold slope implies fewer interface and bulk trap states in/near the channel. For the device without a SiO_x protection layer, photoresist is used as the etching mask for IGZO. Thus, the back channel of IGZO has been exposed to some process chemicals. Yet for the device with a SiO_x protection layer, SiO_x is used as the hard etching mask for IGZO. Thus, the back channel of IGZO can keep the properties intact.

To determine the feasibility of oxide TFTs for large-area production, IGZO TFTs on Gen 6 (1850 \times 1500 mm) glasses were also investigated. The bottom-gate coplanar-type structure without a channel protection layer was used mainly because of its simple process. To fabricate the device, a conventional double-layer metal was first deposited on the cleaned glass substrate, after which it served as the gate electrode. After patterning the gate electrode, a 200-nm silicon oxide (SiO_x) gate insulator layer was formed by PECVD. Then the source and drain electrodes were subsequently formed by depositing the conventional trilayer metal patterned by wet etching. Following the source and drain processes, a 30-nm IGZO active layer was deposited via a DC-type sputtering system with a Gen 6 size target. The growth temperature was kept at room temperature, and the O_2/Ar gas ratio was fixed at about 10%. By providing a suitable oxygen ambient during the depositing process, the deposited IGZO films were to show the properties of a semiconductor and could be used as the active layer. The active layer was then patterned and wet-etched. After that, a SiO_x passivation layer was formed by PECVD, and a contact-layer indium-tin-oxide (ITO) was formed by the DC

sputtering system, respectively. Finally, 250°C post-annealing was processed to improve the device performance. The electrical curves were obtained by measuring the device with a channel width and length of 47.4 and 5.5 μm , respectively. The representative transfer and output characteristics of the fabricated Gen 6 IGZO TFTs are shown in Fig. 4(a) and (b), respectively. The extracted parameters included 5.16 cm^2/Vs field effect mobility, 0.5 V threshold voltage, 0.38 V/decade subthreshold swing, and 1.8×10^8 on/off current ratio. These results show that IGZO TFTs can indeed be fabricated by using the traditional processes in large-area >Gen 6.

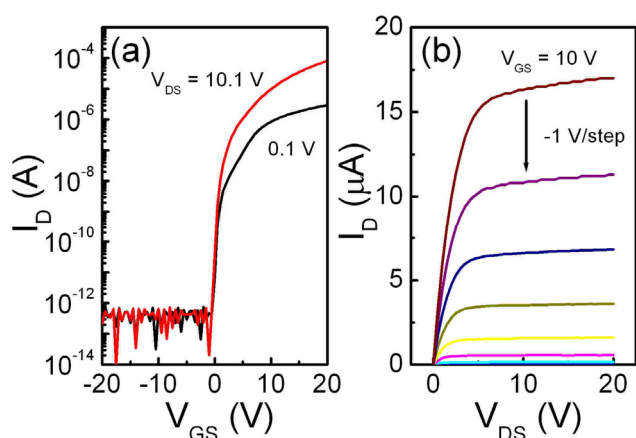


Fig. 4. The representative (a) transfer characteristics and (b) output characteristics of the Gen 6 IGZO TFTs.

3. Flat-Panel Display Applications

3.1 Small AMOLED

As it is plausible that oxide TFTs provide a solution for the AMOLED backplane, AMOLED displays using IGZO TFTs and both normal and inverted OLEDs were demonstrated [14]. In both normal and inverted OLEDs, ITO is used as the bottom transparent conducting electrode. While ITO serves as the anode of the normal OLED, it serves as the cathode of the inverted OLED. The operation voltage of the inverted OLED is typically larger than that of the normal OLED because of the higher electron injection barrier between ITO and the organic layers, such as the electron transport layer on ITO. Fig. 5 shows a picture of a 2.4-inch AMOLED panel with IGZO TFTs and inverted OLEDs. The panel resolution is QVGA (320×RGB×240), whereas each subpixel has a 2T1C circuit design. Despite the higher operation voltage, the image-sticking issue



Fig. 5. A 2.4-inch IGZO TFT AMOLED with an inverted OLED.

caused by the variation of the OLED driving voltage is largely suppressed for the inverted OLED, mainly due to the proper driving scheme.

3.2 Transparent AMOLED

The unique properties of oxide-based semiconductors, such as a wide bandgap and high transparency, also make some novel applications possible. For instance, the objects at the opposite side of a transparent display can be seen, and many interesting applications can thus be created. Here, a see-through-type transparent AMOLED was also fabricated using IGZO TFTs as the active devices and the transparent conducting oxide (TCO) as the electrodes [15]. As uniformity can become an issue in such configuration, the normal OLED is used here instead of the inverted one because of the former's lower operation voltage. As shown in Fig. 6, the 2.4-inch transparent display shows high QVGA trans-



Fig. 6. A 2.4-inch IGZO TFT transparent AMOLED.

parency (45%) and resolution.

3.3 Large AMLCD

Another advantage of oxide TFTs is their capability to be scaled up. Although it was confirmed that IGZO TFTs can be fabricated in the Gen 6 fab using the conventional processes, it is also important to determine the uniformity and reliability of display panels using oxide TFTs, and whether the LCD module processes will damage oxide TFTs. As shown in Fig. 7, the 32-inch IGZO TFT AMLCD was successfully fabricated in the Gen 6 TFT-LCD fab [16]. The display panel is defect- and mura-free, showing the feasibility of using oxide TFTs for such large AMLCD production. Furthermore, such achievement is a very important first step in the development of large AMOLED displays. In short, it was confirmed that such new technology can be realized in a conventional fab that is larger than Gen 6, which will definitely promote large-AMOLED display development.



Fig. 7. A 32-inch IGZO TFT AMLCD.

4. Summary

As a rising star, AMOLED is expected to provide solutions for better-performance displays. AMOLED, however, has stringent demands on the driving TFTs mainly because of its current driving nature. In this paper, several advantages of oxide TFTs are shown, such as high mobility, good uniformity, small hysteresis, and moderate stability. In addition, several IGZO-TFT-driven display prototypes are demonstrated, including a 2.4-inch AMOLED with an inverted

OLED, a 2.4-inch transparent AMOLED with 45% transparency, and a 32-inch AMLCD that proves that such new technology can be scaled up to Gen 6. Thus, it is believed that oxide TFTs can be strong candidates for the next-generation TFT technology for AMOLED and AMLCD.

References

- [1] C. W. Tang and S. A. VanSlyke, *Applied Physics Letters* **51**, 913 (1987).
- [2] C.-C. Wu, C.-W. Chen, C.-L. Lin, and C.-J. Yang, *Journal of Display Technology* **01**, 248 (2005).
- [3] K. Nomura, H. Ohta, K. Ueda, T. Kamiya, M. Hirano, H. Hosono, *Science* **300**, 1269 (2003).
- [4] K. Nomura, H. Ohta, A. Takagi, T. Kamiya, M. Hirano, and H. Hosono, *Nature* **432**, 488 (2004).
- [5] H. Hosono, *Journal of Non-Crystalline Solids* **352**, 851 (2006).
- [6] R. Hayashi, M. Ofuji, N. Kaji, K. Takahashi, K. Abe, H. Yabuta, M. Sano, H. Kumomi, K. Nomura, T. Kamiya, M. Hirano, and H. Hosono, *Journal of the Society for Information Display* **15**, 915 (2007).
- [7] H.-H. Hsieh, T. Kamiya, K. Nomura, H. Hosono, and C.-C. Wu, *Applied Physics Letters* **92**, 133503 (2008).
- [8] H.-N. Lee, J. Kyung, M.-C. Sung, D. Y. Kim, S. K. Kang, S.-J. Kim, C. N. Kim, H.-G. Kim, and S.-T. Kim, *Journal of the Society for Information Display* **16**, 265 (2008).
- [9] J. K. Jeong, J. H. Jeong, H. W. Yang, T. K. Ahn, M. Kim, K. S. Kim, B. S. Gu, H.-J. Chung, J.-S. Park, Y.-G. Mo, H. D. Kim, and H. K. Chung, *Journal of the Society for Information Display* **17**, 95 (2009).
- [10] M. Furuta, M. Kimura, T. Hiramatsu, T. Nakanishi, C. Li, and T. Hirao, *Journal of the Society for Information Display* **18**, 773 (2010).
- [11] H.-H. Hsieh, C.-H. Wu, C.-W. Chien, C.-K. Chen, C.-S. Yang, and C.-C. Wu, *Journal of the Society for Information Display* **18**, 796 (2010).
- [12] S.-H. K. Park, M. Ryu, S. Yang, C. Byun, C.-S. Hwang, K. I. Cho, Woo-Bin Im, Y.-E. Kim, T.-S. Kim, Y.-B. Ha, and K.-B. Kim, in *SID Technical Digest* (2010), p. **245**.
- [13] C. R. Kagan and P. Andry, *Thin-Film Transistors* (Marcel Dekker, New York, 2003).
- [14] H.-H. Hsieh, T.-T. Tsai, C.-Y. Chang, H.-H. Wang, J.-Y. Huang, S.-F. Hsu, Y.-C. Wu, T.-C. Tsai, C.-S. Chuang, L.-H. Chang, and Y.-H. Lin, in *SID Technical Digest* (2010), p. 140.
- [15] H.-H. Hsieh, T.-T. Tsai, C.-Y. Chang, S.-F. Hsu, C.-S. Chuang, and Y. Lin, *Journal of the Society for Information Display*, (accepted).
- [16] H.-H. Lu, H.-C. Ting, T.-H. Shih, C.-Y. Chen, C.-S. Chuang, and Y. Lin, in *SID Technical Digest* (2010), p. 1136.

[Parts of this work were presented in Proceedings of IMID 2010.]